Europhys. Lett., **62** (1), pp. 49–55 (2003)

The self-organized phase of bulk P_xSe_{1-x} glasses

D. G. Georgiev[1], P. Boolchand[1], H. Eckert[2],
M. Micoulaut[3] and K. Jackson[4]

[1] *Department of Electrical and Computer Engineering and Computer Science University of Cincinnati - Cincinnati, OH 45221-0030, USA*
[2] *Institut fur Physikalische Chemie, Westfaelische Wilhelms Universität Münster D-48149 Münster, Germany*
[3] *Laboratoire de Physique Théorique des Liquides, Université Pierre et Marie Curie Boîte 121, 4 Place Jussieu, 75252 Paris, Cedex 05, France*
[4] *Department of Physics, Central Michigan University - Mt. Pleasant, MI 48858, USA*

(received 7 October 2002; accepted in final form 20 January 2003)

PACS. 61.43.Fs – Glasses.
PACS. 62.20.-x – Mechanical properties of solids.

Abstract. – Modulated Scanning Calorimetry shows the non-reversing heat flow near T_g to display a sharply defined global minimum in the $0.28 < x < 0.40$ range, identified with the self-organized phase (SOP) of titled glasses. ^{31}P NMR, Raman scattering and constraint counting algorithms suggest this phase to consist of two distinct global morphologies; a Se-rich backbone that has a dimensionality $2 < d < 3$, and P-rich ribbons that have $d \simeq 1$. The ribbons dominate the physical behavior of stressed rigid ($0.40 < x < 0.50$) glasses with unusual consequences.

New insights into the nature of glass transitions, elastic phases and self-organization of molecular networks have emerged from T-modulated Differential Scanning Calorimetry (MDSC) [1–3]. The method permits separating the endothermic heat flow near T_g into two parts; an ergodic fraction (thermally reversing heat flow, dH_r/dt) and a non-ergodic one (non-reversing heat flow, dH_{nr}/dt). Operationally [4], the separation is achieved by imposing small (1 °C) sinusoidal T oscillations at low frequencies (10^{-2} cps) on a linear T-ramp at slow scan rates (3 °C/min). The reversing heat flow represents that component of heat flow that tracks the T oscillations. Experiments on glasses show that dH_r/dt displays a textbook glass transition on a flat baseline and the inflection point can serve to define T_g, while the step size of the jump gives the thermodynamic change in the specific heat ΔC_p near T_g (fig. 1a). The dH_{nr}/dt term, on the other hand, shows a peak as a precursor to the glass transition, and the integrated area under the peak (shaded area, fig. 1a), ΔH_{nr}, in relaxed bulk glasses [1] provides the relaxation enthalpy. Experiments show that the ΔH_{nr} term ages and saturates with time to yield the configurational entropy change of a relaxed bulk glass as it softens near T_g.

Trends in ΔH_{nr} as a function of global connectivity or mean coordination number, $\bar{r}$, of glass networks have shown [1] the existence of compositional windows across which the term nearly vanishes. These thermally reversing windows are found to correlate well with Raman elastic thresholds [5] and serve to delineate floppy from stressed rigid-glass compositions.

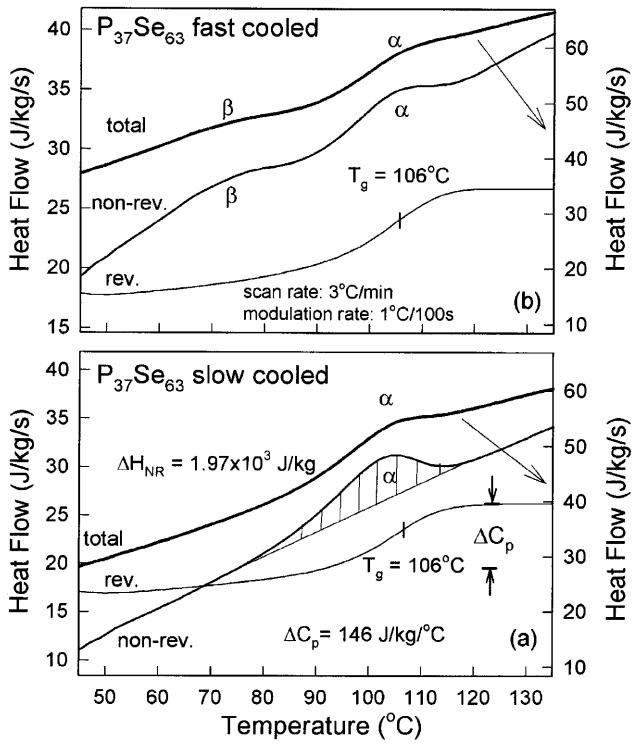

Fig. 1 – MDSC scan of $P_{37}Se_{63}$ glass synthesized by (a) slow cool, (b) fast cool of a melt. The fast-cooled glass is obtained by a water-quench of a melt. The slow-cooled glass here was obtained by cycling the fast-cooled glass through T_g and let relax at room temperature for a week prior to initiating a T-scan up to T_g. Results parallel to those shown in (a) are obtained for a melt air-cooled to room temperature.

These windows have attracted general interest in glass science [1], percolation problems [6] in condensed-matter science including in high-temperature superconductivity [7], protein folding [8], and the traveling-salesman problem in computer science [9]. The windows are identified with intermediate phases in network glasses and represent nearly stress-free self-organized phases (SOPs) of disordered networks [1, 6, 7].

In this letter, we show that in water-quenched P_xSe_{1-x} glasses, the non-reversing heat, $(\Delta H_{nr}(x))$, associated with the T_g endotherm shows a global minimum (fig. 2b) in the $0.28 < x < 0.40$ range with sharply defined edges. The result fixes the SOP in the present glasses. Furthermore, ^{31}P NMR, Raman scattering and constraint counting algorithms show that this phase consists of two distinct morphologies, one of pyramidal $P(Se_{1/2})_3$ and quasi-tetrahedral $Se = P(Se_{1/2})_3$ units with dimensionality $2 < d < 3$, and a second of ribbonlike ethylenelike $P_2(Se_{1/2})_2Se_2$ units with $d = 1$. The morphologies display a high degree of cluster polymerization resulting in the sharp thermal thresholds. A Model 2920 MDSC from TA Instruments Inc. was used to examine the glass transitions. Details of glass synthesis and molecular structure of P-Se glasses were elucidated [10] in Raman scattering and ^{31}P NMR studies. Figure 2a, b and c provide, respectively, compositional trends in $T_g(x)$, $\Delta H_{nr}(x)$ and $\Delta C_p(x)$ for quenched glasses. Measured molar volumes of glasses also appear in fig. 2c. Concentrations of local structural units established [10, 11] from NMR appear in fig. 3a. The $\Delta H_{nr}(x)$ trend of fig. 2b reveals a global minimum in the $0.28 < x < 0.40$ composition range

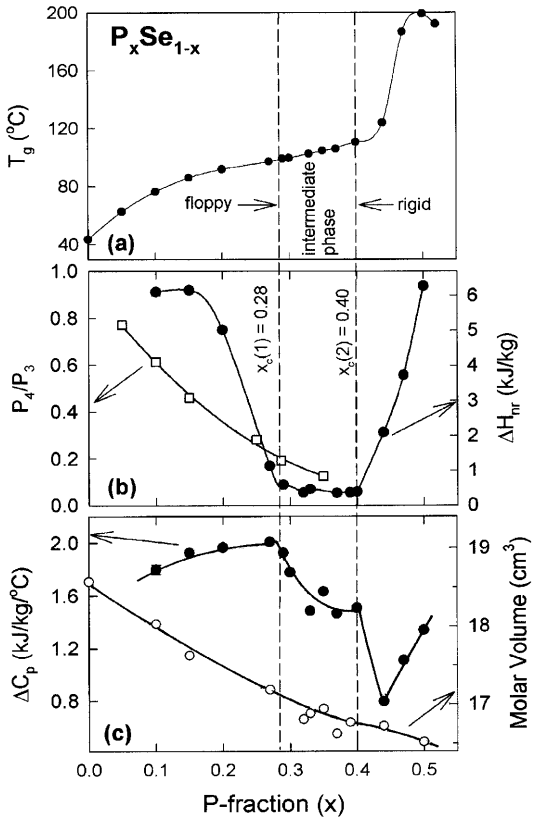

Fig. 2

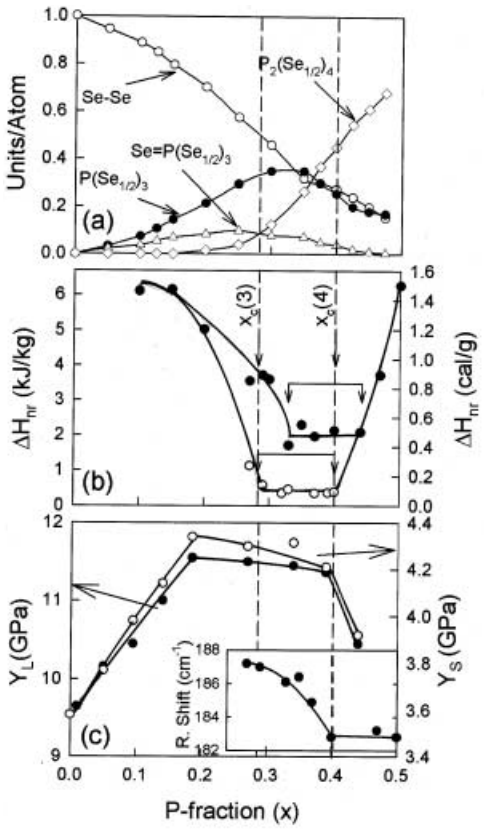

Fig. 3

Fig. 2 – Compositional trends in (a) glass transition temperatures, $T_g(x)$, (b) non-reversing heat flow, $\Delta H_{nr}(x)$ and (c) specific-heat jump $\Delta C_p(x)$ and molar volumes in P-Se glasses. Molar volumes of glasses were measured using Archimedis principle and yield a value of 18.6(1) cm^3 for Se glass and 16.7(1) cm^3 for $P_{40}Se_{60}$ glass. These values are in good agreement with previous reports in the literature. The ratio $P_4/P_3(x)$ taken from ref. [9], is included in panel (b). The interval between the pair of dashed vertical lines gives the intermediate phase.

Fig. 3 – Compositional trends of (a) various molecular units populated in P-Se glasses deduced from ^{31}P NMR results and taken from ref. [8], (b) $\Delta H_{nr}(x)$ in slow-cooled (filled circles) and water-quenched (open circles) glasses, and (c) longitudinal (Y_L) and shear (Y_S) elastic constants taken from ref. [13]. The inset gives the compositional trend of the Raman mode frequency of ethylenelike chains, showing a kink near $x = 0.40$.

where T_g's become almost completely thermally reversing. Glass samples produced by slow-cooling melts (3 °C/min) or by cycling through T_g, and let relax at room temperature for several days prior to MDSC scans, show only one endotherm (fig. 1a) uniformly, however. In such slowly cooled samples $\Delta H_{nr}(x)$ trend shows a narrower and shallower global minimum (fig. 3b). Furthermore, trends in Youngs moduli ($Y_L(x)$) and shear moduli ($Y_S(x)$) of these glasses [12] display mesas (fig. 3c) with kinks near $x = 0.18$ and 0.40.

Our interpretation of these results is as follows. The observation of a thermally reversing window [1–3, 5] in the $0.28 < x < 0.40$ composition range suggests that it represents the SOP, the compositions $x < 0.28$ mechanically floppy ($n_c < 3$), while those at $x > 0.40$ stressed

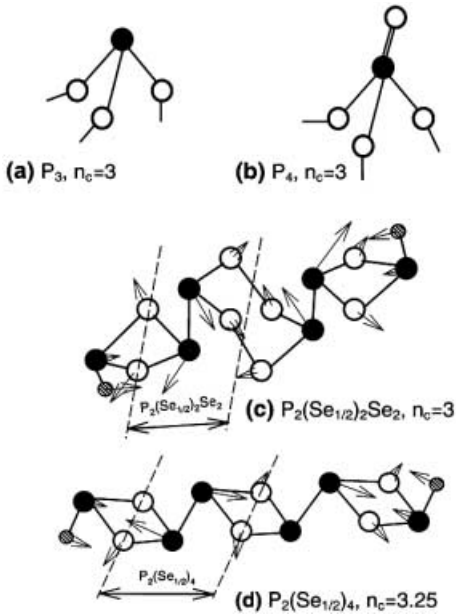

Fig. 4 – (a) Pyramidal $P(Se_{1/2})_3$; (b) quasi-tetrahedral $Se = P(Se_{1/2})_3$ units; (c) $P_2(Se_{1/2})_2Se_2$ and (d) $P_2(Se_{1/2})_4$ cluster models used in the density functional theory calculations. Filled and open circles represent P and Se atoms, respectively, the smaller, shaded circles represent H atoms used for cluster termination. The arrows represent the eigenvectors of the ring-pinching vibrational modes.

rigid ($n_c > 3$) in the present glasses. Of special interest are the 4- and 3-fold coordinated P-units (labeled as P_4 and P_3 in fig. 4a and b), and $P_2(Se_{1/2})_2Se_2$ ribbons (fig. 4c). A count of Lagrangian bonding constraints per atom (n_c) due to bond-stretching and bond-bending forces shows [3, 13] that each of these units is isostatically rigid ($n_c = 3$), and for that reason they must comprise elements of local structure of the SOP. Furthermore, for rigidity to percolate in a network it must do so at all length scales [8]. The requirement fixes acceptable medium-range structures. The P_3 and P_4 units most likely exist in rings that are interconnected to form a network with a dimensionality in the $2 < d < 3$ range. On the other hand, the $P_2(Se_{1/2})_2Se_2$ units form quasi-1d ribbons (fig. 4c). We believe that there are thus two distinct morphologies, one with $2 < d < 3$, and the other with $d = 1$ as the medium-range structures of the SOP.

Recent Raman [10] and NMR [11] results identify local glass structures in the present binary. At low x (< 0.10), isolated P_4 (fig. 4a) and P_3 (fig. 4b) units stochastically crosslink [14] the Se_n-chain network that is reflected in a $T_g(x)$ increase (fig. 2a) as well as an elastic-moduli ($Y_{L,S}(x)$) (fig. 3c) increase. The $T_g(x)$ increase at low x (< 0.10) is quantitatively described [10] in terms of the stochastic agglomeration theory. At higher x (> 0.10), P_4 and P_3 units coalesce to nucleate isostatically rigid fragments in the floppy phase, and $Y_{L,S}(x)$ continue to increase. The continued growth of these fragments is however stymied by nucleation [10] of P-rich ribbons (fig. 3a) near $x > 0.15$. The result is a kink in $Y_{L,S}(x)$ near $x = 0.18$ leading to a flat variation thereafter, reflecting a kind of Van-Hove–Phillips saddle point singularity [15]. With a further increase of x, P_4- and P_3-bearing rigid fragments steadily grow (fig. 3a) as do the lengths of the rigid $P_2(Se_{1/2})_2Se_2$ ribbons (fig. 4c), and the first percolative rigidity transition onsets near $x = 0.28$. In the SOP two distinct morphologies appear whose relative concentrations change across that phase. These morphologies do not mix accounting for the near absence of the ΔH_{nr}-term in the SOP. The novelty of the SOP is that it is not predicted

by standard mean-field theory [6, 7] of random networks. The phase is formed on energetic grounds in which population of these select stress-free structures lowers the free energy of melts to self-organize the glassy networks. The SOP is unlike any other phase encountered in glasses to date and represents a paradigm of self-organization of complex networks [16] at a systems level to include biological, electrical and mechanical networks.

With increasing x (> 0.40) the stressed rigid phase manifests itself, and consists of over-constrained ($n_c = 3.25$) P-rich $P_2(Se_{1/2})_4$ quasi-1d ribbons (fig. 4d). In Raman scattering a vibrational mode of these ribbons appears [10] near $185\,cm^{-1}$, which displays a sharp kink near $x = 0.40$ (fig. 3c, inset), whose microscopic origin is elucidated by cluster calculations next.

First-principles density functional calculations [17, 18] of vibrational modes in geometry-optimized, H-terminated clusters of fig. 4c and d were undertaken. These calculations show that the 4-member $P_2(Se_{1/2})_4$ rings are stable only in a non-planar geometry, in harmony with the established [19] crystal structure of α-P_4Se_4. Furthermore, the calculations reveal a series of modes at frequencies greater than $300\,cm^{-1}$, ring-stretching modes that are also observed [10] in Raman scattering. But of special interest is a ring-pinching mode predicted by these calculations (eigenvectors shown in fig. 4c) that is found to red-shift from $175\,cm^{-1}$ in the cluster of fig. 4c to $172\,cm^{-1}$ in the cluster of fig. 4d. The removal of Se from the 6-member rings of the fig. 4c cluster, converts them to 4-member ones of the fig. 4d cluster. The observed red-shift of the $185\,cm^{-1}$ mode parallels that of the cluster calculations above to suggest that it constitutes signature of Se depletion of the isostatic ribbons (fig. 4c) to render them stressed rigid (fig. 4d) as the second rigidity transition manifests near $x = 0.40$. The Raman results also correlate well with the sharp transition [12] in $Y_{L,S}(x)$ near $x = 0.40$ to suggest that the underlying phase transition is probably first order in character and in harmony with recent numerical simulations [20].

There is a surprise, however. Numerical [6] and experimental [1, 5] results on 3d networks have hitherto shown elasticity to increase as a function of mean coordination number, $\bar{r}$, as a power law in stressed rigid phases of Ge-Se [5] and Si-Se [21] glasses. On the other hand, in the present glasses the elasticity [12] is found to sharply decrease (fig. 3c) in the stressed rigid phase ($x > 0.40$). The increased global connectivity of glasses in the $0.40 < x < 0.50$ range is confirmed by the sharp increase of T_g (fig. 2a) which derives from growth of the stressed rigid ribbons at the expense of the residual Se-rich phase. The $d = 1$ nature of the stressed rigid ribbons leads not only to lower molar volumes at $x > 0.40$ (fig. 2c) as ribbons pack well, but also to an unprecedented reduction in shear elasticity (fig. 3c) as ribbons slide past each other.

The observation of a sub-T_g endotherm in water-quenched samples (fig. 1b) but not in slow-cooled ones or in glasses cycled through T_g (fig. 1a) deserves a final comment. The sub-T_g endotherm is centered near $77\,^\circ C$, and has a heat of transformation of about $0.2\,cal/gm$. Sub-T_g endotherms have been observed [22] in polymers using mechanical and dielectric loss spectroscopies and are usually identified with thermal activation of side-chains to a backbone. ^{31}P NMR results [23] on binary P_xSe_{1-x} liquids have shown a thermally activated conversion of P_4-units into P_3 ones by the following exothermic reaction:

$$Se = P(Se_{1/2})_3 \longrightarrow P(Se_{1/2})_3 + Se_n. \tag{1}$$

The reaction equilibrium shifts to the right in melts at higher temperatures as some excess Se_n is progressively released. Upon a water quench, the excess Se is frozen in the glasses, and as the temperature of such glasses is increased, the excess Se irreversibly reacts with P_3-units to convert them to P_4 near $77\,^\circ C$, accounting for the origin of the sub-T_g endotherm. The endotherm represents an activation energy and remains largely constant in the $0.28 < x < 0.40$ range because the P_3/P_4 ratios in glasses (obtained by a quench near the liquidus T_l, see fig. 3a)

do not change appreciably with x in the range of interest. However, in glasses quenched well above T_l, we find $\Delta H_\mathrm{nr}(x)$ term to decrease, thus confirming the microscopic origin of the sub-T_g endotherm.

In summary, the general feature of rigidity onset exemplified by the P_xSe_{1-x} glasses is that there are two transitions, a global one at $x = 0.40$, and a local one at $x = 0.28$ that serve to define the SOP. Two highly polymerized morphologies, one with $2 < d < 3$, and the other with $d = 1$ coexist in the SOP but do not mix, and is reflected in the thermally reversing character of the T_g's and the sharpness of the thermally reversing window.

* * *

This work is supported by NSF grants DMR-01-010808 (University of Cincinnati) and DMR-RUI-9972333 and DMR-MRI-9977582 (Central Michigan University). LPTL is Unité Mixte de Recherche CNRS No. 7600.

REFERENCES

[1] Boolchand P., Georgiev D. G. and Goodman B., *J. Optoelectron., Adv. Mater.*, **3** (2001) 703. Aging effects are also observed in the ΔH_nr term that apparently saturates when glasses are relaxed below T_g for extended periods, see also Boolchand P., Georgiev D. G. and Micoulaut M., *J. Optoelectron., Adv. Mater.*, **4** (2002) 823.

[2] Georgiev D. G., Boolchand P. and Micoulaut M., *Phys. Rev. B*, **62** (2000) R9228.

[3] Wang Y., Boolchand P. and Micoulaut M., *Europhys. Lett.*, **52** (2000) 633; Boolchand P. and Bresser W., *Nature*, **410** (2001) 1070.

[4] Wunderlich B., Jin Y. and Boller A., *Thermochim. Acta*, **238** (1994) 277. See also Modulated DSC, document TA210, T.A. Instruments, Inc., New Castle, DE, `http://www.tainst.com`.

[5] Boolchand P., Feng X. and Bresser B, *J. Non-Cryst. Solids*, **293-295** (2001) 348.

[6] Thorpe M. F. and Chubinsky M. V., *Phase Transitions and Self-Orgamization in Electronic and Molecular Networks*, edited by Phillips J. C. and Thorpe M. F. (Kluwer Academic/Plenum Publishers) 2001, p. 43.

[7] Phillips J. C., *Philos. Mag.*, **80** (2000) 1773. Also see Phillips J. C., *Phys. Rev. Lett.*, **88** (2002) 216401.

[8] Rader A. J., Hespenheide M. B., Kuhn L. A. and Thorpe M. F., *Proc. Natl. Acad. Sci.*, **909** (2002) 3540.

[9] Monasson R., Zecchina R., Kirkpatrick S., Selman B. and Toyansky L., *Nature*, **400** (1999) 133.

[10] Georgiev D. G., Mitkova M., Boolchand P., Brunklaus G., Eckert H. and Micoulaut M., *Phys. Rev. B*, **64** (2001) 134204.

[11] Lathrop D. and Eckert H., *Phys. Rev. B*, **43** (1991) 7279.

[12] Orlova G. M., Zigel V. V., Chalabyan G. A. and Lavreneva O. S., *Fiz. Khim. Stekla*, **1** (1975) 354. Also see Borisova Z. U., *Glassy Semiconductors* (Plenum Press, New York) 1981, p. 81.

[13] For an atom possessing a coordination number r, the number of bond-stretching constraints $n_\alpha = r/2$, while the number of bond-bending constraints $n_\beta = 2r - 3$. For the $P(Se_{1/2})_3$ unit: $n_\mathrm{c}(\mathrm{P}) = 3/2 + 3$, $n_\mathrm{c}(\mathrm{Se}) = 2$, thus (2.5) $n_\mathrm{c} = 4.5 + 3 = 7.5$ or $n_\mathrm{c} = 3$. For the $Se = P(Se_{1/2})_3$ unit: $n_\mathrm{c}(\mathrm{P}) = 7$, $n_\mathrm{c}(\mathrm{nb\text{-}Se}) = 1/2$, $n_\mathrm{c}(\mathrm{Se}) = 2$, thus (3.5) $n_\mathrm{c} = 7 + 1/2 + 3 \times 1/2 \times 2 = 10.5$ or $n_\mathrm{c} = 3$. For treatment of non-bridging (nb) or dangling ends, see Boolchand P. and Thorpe M. F., *Phys. Rev. B*, **50** (1994) 10366.

[14] Kerner R. and Micoulaut M., *J. Non-Cryst. Solids*, **210** (1997) 298.

[15] Phillips J. C., *Phys. Rev.*, **104** (1956) 1263. Van Hove L., *Phys. Rev.*, **89** (1953) 1189.

[16] Kitano H., *Science*, **295** (2002) 1662. There are several papers relating to Systems Biology in the same issue.

[17] Jackson K., Briley A., Grossman S. and Porezag D. V., *Phys. Rev. B*, **60** (1999) R14985.
[18] Pederson M. R. and Jackson K. A., *Phys. Rev. B*, **41** (1990) 7453.
[19] Ruck M., *Z. Anorg. Allg. Chem.*, **620** (1994) 1832.
[20] Thorpe M. F., Jacobs D. J., Chubinsky M. V. and Phillips J. C., *J. Non-Cryst. Solids*, **266-269** (2000) 872.
[21] Selvanathan D., Bresser W. J. and Boolchand P., *Phys. Rev. B*, **61** (2000) 15061.
[22] Menard K. P., *Dynamic Mechanical Analysis* (CRC Press, Washington, DC) 1999, p. 95 and references therein.
[23] Maxwell R. and Eckert H., *J. Am. Ceram. Soc.*, **116** (1994) 682.